



Prediction of speed limit of cars moving on corroded steel girder bridges using artificial neural networks

NGOC-LONG TRAN, DUY-DUAN NGUYEN and TRONG-HA NGUYEN*

Department of Civil Engineering, Vinh University, Vinh 461010, Vietnam
e-mail: trongha@vinhuni.edu.vn

MS received 16 January 2022; revised 21 April 2022; accepted 10 May 2022

Abstract. This paper develops an artificial neural network (ANN) model for predicting the speed limit of cars moving on corroded steel girder bridges. A total of 311 datasets, which are created from the proposed analytical model, are used to construct the ANN model. The input parameters of the proposed ANN model include the car's weight, diameter of tires, and the dimensions of girder bridges, which are the top flange width, top flange thickness, bottom flange width, bottom flange thickness, girder height, web thickness, and the span of girder. Meanwhile, the speed limit of cars is the output variable of the ANN model. The results show that the speed limitation of cars on the corrosive steel girder bridge is reduced pronounced after 100 years. Sensitivity analyses reveal that the influential parameters with respect to the maximum speed are the girder height and tire diameter, whereas the girder weigh and girder span have negative effects on the speed limit of cars. Moreover, a mathematical formula and a graphical user interface program are developed to calculate the speed limits of cars on the corrosive steel girder bridge. These practical tools are very helpful for practitioners in determining the speed limit of cars moving on steel girder bridges subjected to corrosion.

Keywords. Artificial neural network; corroded steel girder bridges; speed limits; predictive formula; graphical user interface.

1. Introduction

Speed limit is the one of crucial parameters for improving the traffic safety. Especially, the service life of traffic works is degraded by time due to environmental factors. The steel girder bridges are widely used in traffic structures since its simple construction. However, this structure is corroded by time, and therefore the speed limit of cars should be carefully considered.

Corrosion is a complicated phenomenon, which is normally expressed in terms of mathematical formulations. Komp [1] proposed a typical corrosion model considering different types of environments such as marine, urban and rural areas. Landolfo *et al* [2] conducted a systematic literature review on the damaged modeling of metal structures subjected to corrosions. In the study of Seccer *et al* [3], they employed Komp model to figure out the corroded failure of steel frames accounting for lateral bending. Nguyen and Nguyen [4] assessed the reliability of steel-concrete composite beams after 100 years considering Komp model and sensitivity analyses. In addition, reliability analyses of steel structures accounting for the effects of corrosion were studied numerously [5–7]. However, a study on the speed limit of cars on the steel girder bridge

considering corrosion effects is not systematically investigated so far.

Over the last few decades, the artificial intelligence (AI) techniques have been widely applied for various engineering problems, in which the artificial neural network (ANN) model is one of the most popular methods [8–11]. Regarding traffic engineering, ANN was employed for predicting the driver behavior, vehicle detection [12], damage detection [13], traffic pattern analysis [14], traffic flows measurement [15, 16], pavement maintenance [17], classification of vehicle detection [18], and traffic control [19]. Additionally, ANN technique was also applied for cargo activity, prediction accident scenario, economics and transport policy, air transport, and sea transportation [14]. Nevertheless, to the best of the authors' knowledge, there is no study applying any AI models such as ANN to predict the maximum speed of cars passing across the corroded steel girder bridge.

Therefore, this study develops a procedure for predicting the speed limit of cars passing on the steel girder bridge considering metal corrosion based on ANN combined with a corrosion model suggested in previous works [1, 20]. For training ANN models, a total of 311 data samples is generated based on the analytical model. Input parameters of the proposed ANN model are the car's weight (M), diameter of tires (DC), and dimensions of steel girder bridges,

*For correspondence
Published online: 15 June 2022

which are the top-flange width (TF), top-flange thickness ($t - TF$), bottom-flange width (BF), bottom-flange thickness ($t - BF$), girder height (D), web thickness ($t - w$), and the girder span (L). Meanwhile, the speed limit of cars ($V_{th(\min)}$) is the output variable of the ANN model. The influence of input variables on the $V_{th(\min)}$ value is evaluated. Finally, practical tools including a mathematical equation and a graphical user interface are developed based on MATLAB [21] for convenient design practices.

2. Calculation model for speed limit of cars moving on steel girder bridges

Considering a car passing on the steel girder bridge, as shown in figure 1, following parameters are included:

- Car's weight (M)
- Diameter of tires (DC)
- Top-flange width (TF)
- Top-flange thickness ($t - TF$)
- Bottom-flange width (BF)
- Bottom-flange thickness ($t - BF$)
- Height of girder (D)
- Web thickness ($t - w$)
- The girder span (L)

The calculated model for the speed limit of cars moving on the simply supported beam can be modeled by the illustration in figure 2. The moving load on the bridge has the following form, as shown in Eq. (1)

$$P(t) = P + G \sin rt \tag{1}$$

The differential equation of the deflection at the center point of the bridge is expressed by Eq. (2)

$$y''(t) + \omega^2 y(t) = \omega^2 \delta_{11} (P + G \sin rt) \sin \theta t \tag{2}$$

The solution of the left side of Eq. (2) has the form:

$$y(t) = A \sin \omega t + B \cos \omega t + \frac{P \delta_{11} \sin \theta t}{1 - \frac{\theta^2}{\omega^2}} \tag{3}$$

else

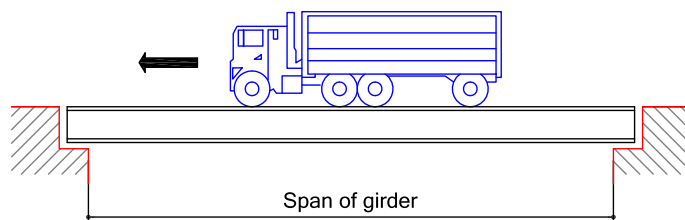
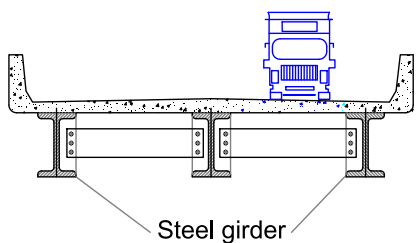


Figure 1. A car moving on the simply supported steel girder bridges.

$$y(t) = A \sin \omega t + B \cos \omega t + \frac{2P}{mL} \frac{\sin \theta t}{\omega^2 - \theta^2} \tag{4}$$

where $\omega^2 = \frac{1}{M \delta_{11}}$ is the natural frequency of the girder; m is the girder mass; $\delta_{11} = \frac{L^3}{48EI}$ is the static displacement of the mass due to unit P ; G is the amplitude of inertia forces of a moving car.

Transforming the right side of Eq. (2), we have

$$\begin{aligned} \omega^2 \delta_{11} G \sin rt \sin \theta t &= \frac{2G}{mL} \sin rt \sin \theta t \\ &= \frac{G}{ml} (\sin \varphi_1 t + \sin \varphi_2 t) \end{aligned} \tag{5}$$

Here, $\varphi_1 = r - \theta$; $\varphi_2 = r + \theta$; $\theta = \frac{pv}{L}$

Rewriting Eq. (2), obtained as follows

$$y''(t) + \omega^2 y(t) = \frac{G}{mL} (\sin \varphi_1 t + \sin \varphi_2 t) \tag{6}$$

The solution of the differential equation in Eq. (6) is

$$y(t) = \frac{G}{mL} \left(\frac{\cos \varphi_1 t}{\omega^2 - \varphi_1^2} + \frac{\cos \varphi_2 t}{\omega^2 - \varphi_2^2} \right) \tag{7}$$

Combining Eq. (4) and Eq. (7), the static deflection of the beam at a setting point is obtained as

$$\begin{aligned} y(t) &= A \sin \omega t + B \cos \omega t + \frac{2P}{mL} \frac{\sin \theta t}{\omega^2 - \theta^2} \\ &+ \frac{G}{mL} \left(\frac{\cos \varphi_1 t}{\omega^2 - \varphi_1^2} + \frac{\cos \varphi_2 t}{\omega^2 - \varphi_2^2} \right) \end{aligned} \tag{8}$$

where A and B are integral constants, which are defined at $t = 0$, then $y(0) = 0$; $y'(0) = 0$, respectively. Then, Eq. (8) can be rewritten as

$$\begin{aligned} y(t) &= \frac{2P}{mL(\omega^2 - \theta^2)} \left(\sin \theta t - \frac{\theta}{\omega} \sin \omega t \right) \\ &+ \frac{G(\cos \varphi_2 t - \cos \omega t)}{mL(\omega^2 - \varphi_1^2)} + \frac{G(\cos \varphi_2 t - \cos \omega t)}{mL(\omega^2 - \varphi_2^2)} \end{aligned} \tag{9}$$

Based on Eq. (9), a resonance occurs in the following cases:

- Case 1: $\omega = \theta$

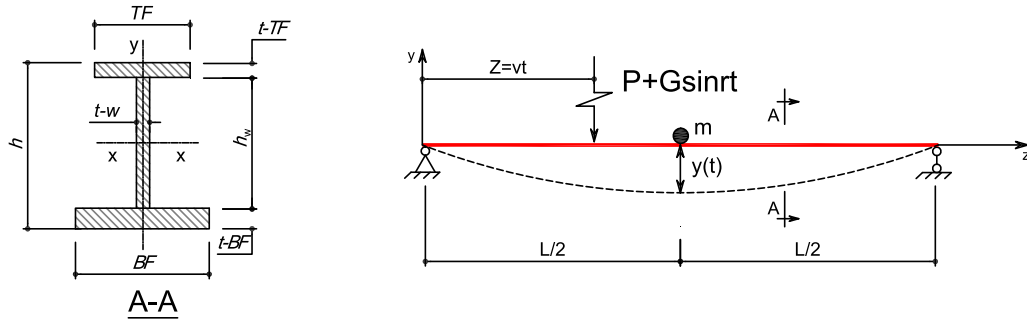


Figure 2. Calculated model of a moving load on the simply supported beam.

- Case 2: $\omega = \varphi_i; (i = 1, 2)$

We have $\omega = \frac{2v_{th}}{DC} \pm \frac{\pi v_{th}}{L}$

The speed limits for the case of moving loads considering the eccentric mass of the car moving on the bridge are

$$v_{th} = \frac{\omega}{\frac{2}{DC} \pm \frac{\pi}{L}} \text{ where } \omega = \frac{\pi^2}{L^2} \sqrt{\frac{EI}{m}} \quad (10)$$

The speed limit is determined by

$$V_{th(min)} = \frac{\omega}{\frac{2}{DC} + \frac{\pi}{L}} \quad (11)$$

where DC is the diameter of the tires.

The calculated model for determining the speed limit is constructed using input parameters consisting of the car’s weight, diameter of tires, and the steel girder bridge configurations based on MATLAB.

3. Dataset generation

To generate data samples, various scenarios of cars moving on the steel girder bridges are considered. A wide range of input parameters comprising of car’s weight (M), tire diameter (DC), and the steel girder bridge dimensions,

which are the top-flange width (TF), top-flange thickness ($t - TF$), bottom-flange width (BF), bottom-flange thickness ($t - BF$), girder height (D), web thickness ($t - w$), and girder span (L), are varied to obtain the speed limit of car. Meanwhile, the speed limit value is determined based on Eq. (11). Finally, a set of 311 datasets is created for training ANN models. The statistical description of the input and output parameters is shown in table 1. The probability distribution of input and output parameters is shown in figure 3.

Figure 4 shows the correlation between input variables and output parameter. It can be seen that the largest correlation between the car’s weight and the bottom flange width is 0.122, while the maximum correlation between the bottom flange width and the output variable is only 0.312. This confirms predicting the speed limit of cars moving on the steel girder bridges with these input and output parameters even more meaningful.

4. The proposed ANN model

4.1 ANN model

So far, ANN has been widely used in various aspects of engineering [22–27]. ANN is a simulation algorithm that

Table 1. The statistical description of the input and output parameters.

Parameter	Units	Minimum	Mean	Maximum	Standard deviation (SD)	Coefficient of variation (CoV)
TF	cm	15.00	42.8810	70.00	14.1470	0.3300
$t-TF$	cm	2.00	5.0958	8.00	1.9409	0.3809
BF	cm	15.00	39.1061	75.00	17.8396	0.4562
$t-BF$	cm	2.00	4.0500	6.00	1.3117	0.3239
D	cm	25.00	69.3087	100.00	20.6293	0.2976
$t-W$	cm	3.00	4.7082	6.00	1.0205	0.2167
M	kG	1000.00	5160.7717	8500.00	1682.4151	0.3260
DC	cm	35.00	78.9068	110.00	16.3064	0.2067
L	cm	1000.00	1961.4148	2500.00	363.9256	0.1855
$V_{th(min)}$	km/hr	12.11	99.3746	577.49	86.0388	0.8658

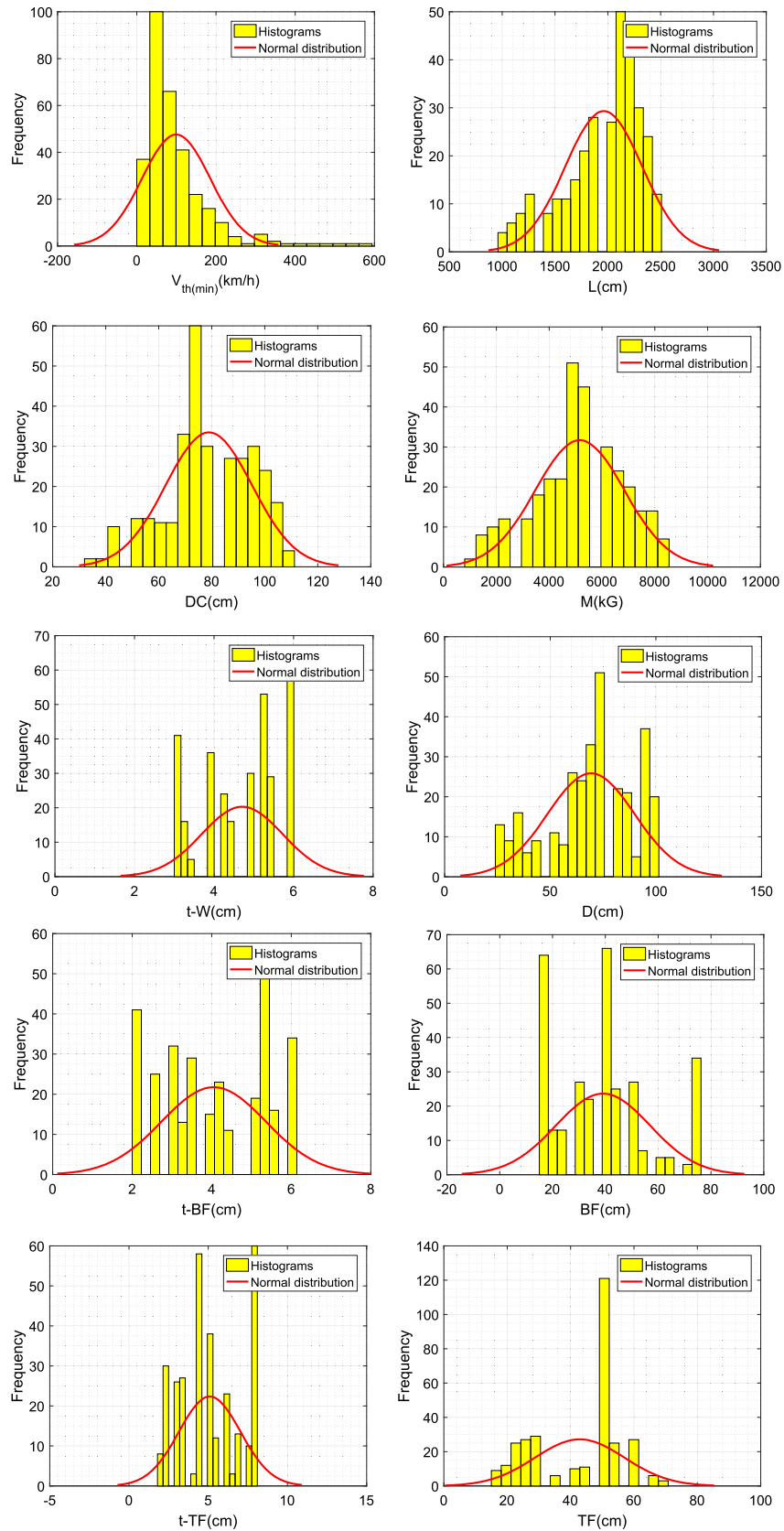


Figure 3. The probability distribution of input and output parameters.

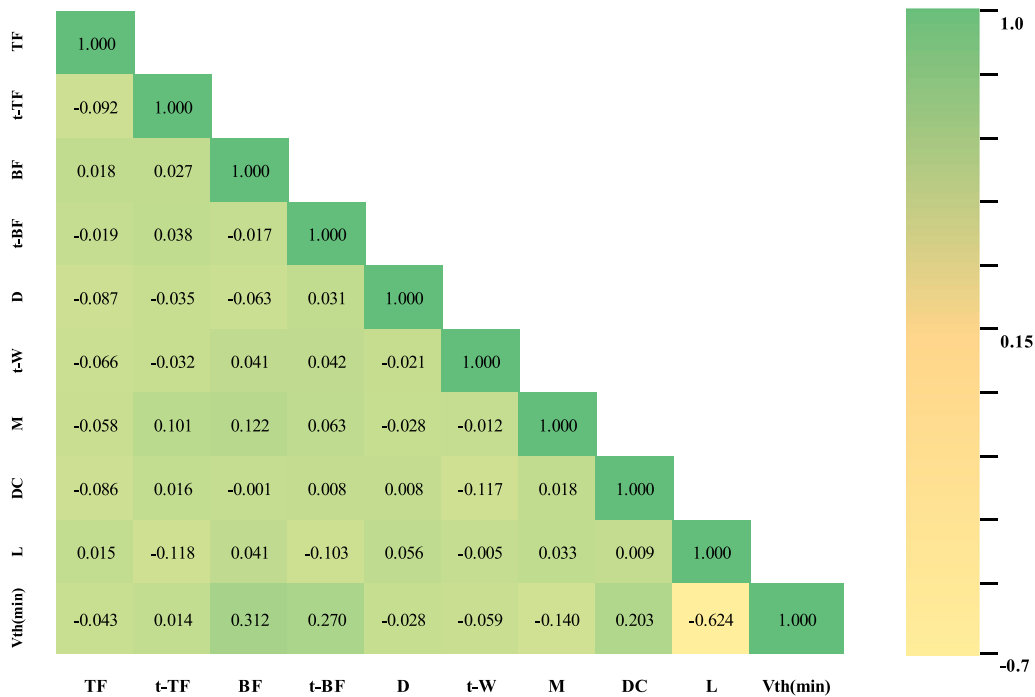


Figure 4. Correlation between input variables and output parameters.

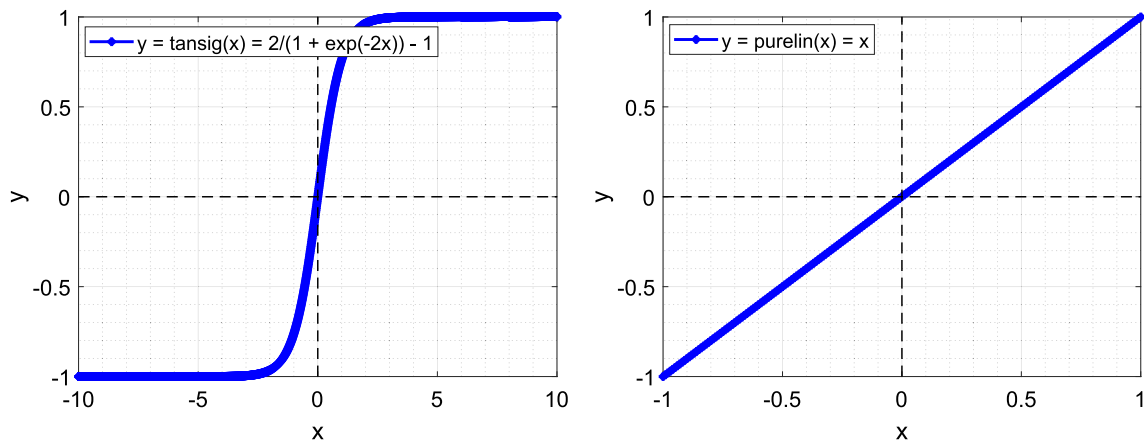


Figure 5. Activation functions: tansig (left) and purelin (right).

mimics the thinking and reasoning of the human brain. This study adopts the back propagation neural network and the Levenberg-Marquardt algorithm with a structure of three layers (i.e., input layer, hidden layer, and output layer). The input layer, hidden layer, and output layer are connected through weights and biases. Its mathematical expression has the form as.

$$f : X \in R^D \rightarrow Y \in R^1 f(X) = f_0(b_2 + W_2(f_h(b_1 + W_1X))) \tag{12}$$

where b_1 , W_1 , and f_h are the biases vector, the weight matrix and the activation function of the hidden layer, respectively. Meanwhile, b_2 , W_2 , and f_0 are the biases vector, the weight matrix and the activation function of the hidden layer output layer, respectively.

The hidden layer activation function used in this study is a nonlinear function (tansig function). And linear function (purelin function) has been used for the output layer [28]. The equation represents the activation function tansig in Eq. (13) and purelin in Eq. (14) and shown in figure 5.

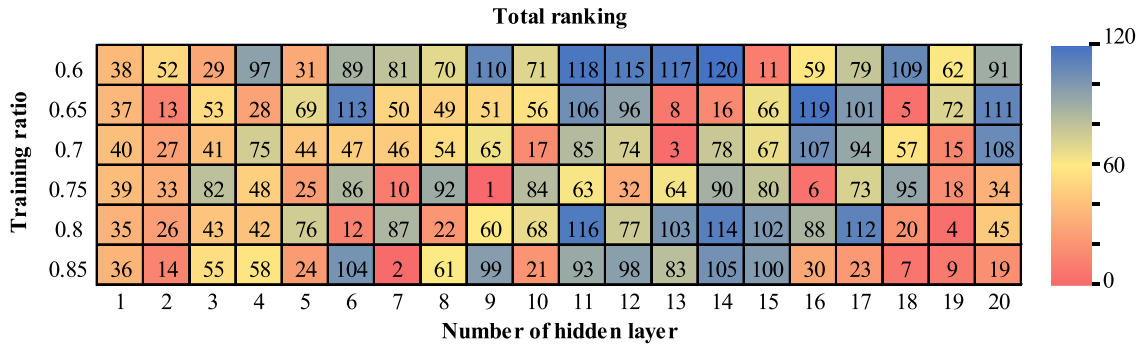


Figure 6. Ranking matrix of 120 proposed ANN structures.

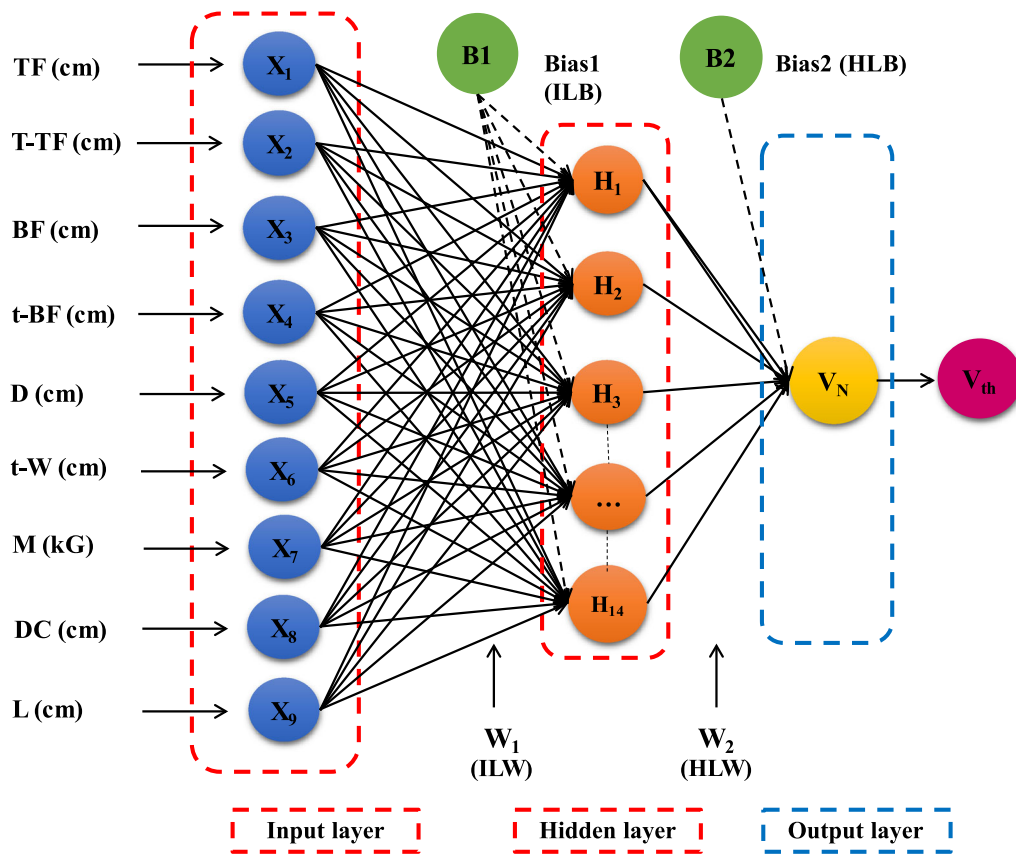


Figure 7. The proposed ANN model structure.

$$tansig(x) = \frac{2}{(1 + \exp(-2x))} - 1 \quad (13)$$

$$purelin(x) = x \quad (14)$$

$$X_n = 2 \times \frac{(X - X_{min})}{(X_{max} - X_{min})} - 1 \quad (15)$$

According to Golafshani & Ashour [29], during the training of the network, the input and output data must be normalized in the interval [-1, 1]. The normalization is shown in Eq. (15).

where X_n is the normalized sample, X_{max} , X_{min} and X are the maximum, minimum and value of the sample under consideration, respectively. The normalized value has into the proposed ANN model and developed by the MATLAB tool.

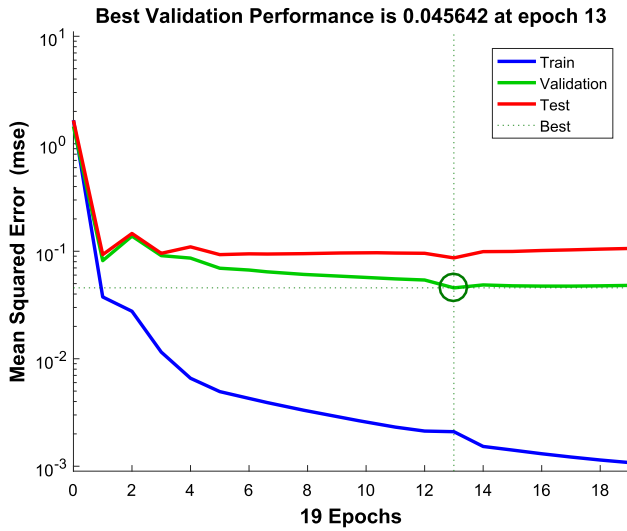


Figure 8. Performance of proposed ANN model.

The process of training the network of continuous feedback loops is performed. To stop the training, the mean square error (*MSE*) was used. The *MSE* is expressed by the following equation.

$$MSE = \min_{b_1, b_2, W_1, W_2} \frac{1}{N} \sum_{i=1}^N e_i^2 \tag{16}$$

where e_i is the deviation of the output layer data and the experimental data; N is number of samples were included in the ANN model.

4.2 Optimization of the proposed ANN model

An ANN model achieves the best performance at the split ratio (training, testing, and validation) combined with the number of hidden layers. To evaluate the best model, three indices, which are coefficient of determination (R^2), root mean squared error (*RMSE*), and *a20-index* were included in the evaluation as suggested by Zorlu *et al* [24]. The equations for determining R^2 , *RMSE*, and *a20-index*, respectively, are as follows.

$$R^2 = 1 - \left(\frac{\sum_{i=1}^n (t_i - o_i)^2}{\sum_{i=1}^n o_i^2} \right); \tag{17}$$

$$RMSE = \sqrt{\left(\frac{1}{n} \right) \sum_{i=1}^n (t_i - o_i)^2}; \tag{18}$$

$$a20 - index = \frac{m20}{n} \tag{19}$$

where t_i is the i^{th} value of the experimental data; o_i is the i^{th} value of the predicted value of ANN model; n is the number of samples; $m20$ is the number of samples with the ratio of the experimental value to the predicted value between 0.8–1.0.

In this study, 120 ANN structures are performed with 06 training ratios including 0.6, 0.65, 0.70, 0.75, 0.8, and 0.85, the test and validation ratios are equal, respectively. Meanwhile, the number of neurons in the hidden layer has been changed from 1 to 20. The best performing model is the model with the highest ranking of R^2 , *RMSE*, and *a20-index*. The ranking results of all the models are shown in figure 6. It can be seen that the training, testing, and validation ratios of the best model are 0.6, 0.2, and 0.2, respectively. Moreover, the optimal model contains 14 neurons in the hidden layer, as shown in figure 7.

4.3 Performance of ANN model

The training results of the ANN model are shown in figure 8 and table 2. It can be seen that the training converges at the 13th epoch with *MSE* of 0.045642. This confirms that the proposed ANN model has been trained very well with the input data.

Figure 9 shows the regression ratio the predicted of the ANN model and the input dataset. The R^2 values of training, testing, and validation data are 0.98076, 0.97071, and 0.98096, respectively. It is close to 1.0. This result implies that the proposed ANN model structure is reliable for predicting the speed limit of cars moving on the steel girder bridge.

Table 2 shows the results of R^2 , *RMSE*, and *a20-index*, and statistical properties (i.e., minimum, maximum, mean,

Table 2. Performance of ANN model.

	R^2	RMSE (km/hr)	a20-index	$V_{th(min)} / V_{th(min)}^{prediction}$				
				Min	Mean	Max	SD	CoV
Training	0.9807	25.497	0.8877	0.510	1.041	1.399	0.126	0.121
Testing	0.9707	30.243	0.8419	0.619	0.924	1.429	0.150	0.162
Validation	0.9809	27.983	0.8710	0.602	0.905	1.485	0.147	0.163
All data	0.9708	60.542	0.8553	0.510	1.010	1.485	0.146	0.145

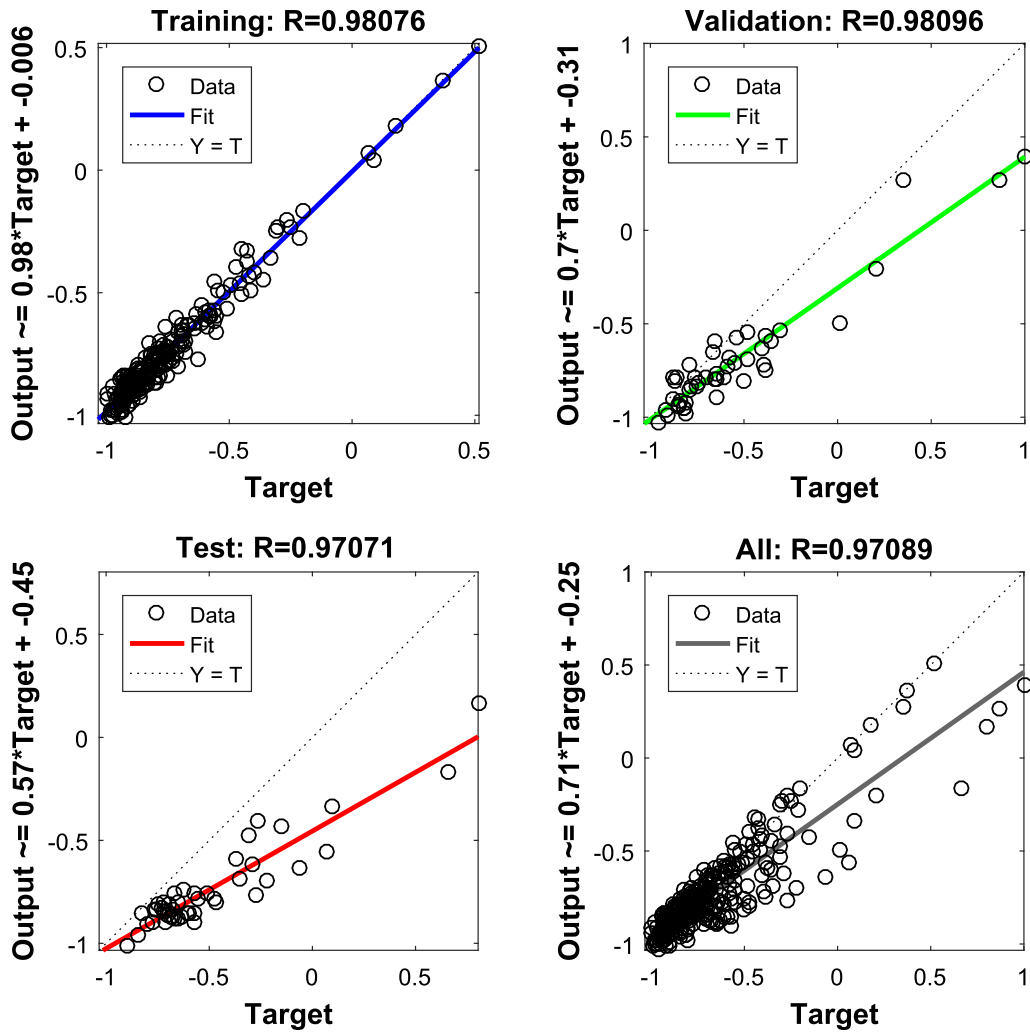


Figure 9. Regression the predicted of the ANN model and the input dataset.

Table 3. Coefficient Δ_A and Δ_B for different environment [1].

Environment	Carbon steel	
	Δ_A	Δ_B
Rural	34.0	0.65
Urban	80.2	0.59
Marine	70.6	0.79

SD, and CoV) of the predicted/dataset ratio. It can be seen that the mean value is very close to 1.0. Once again, it emphasizes that the proposed ANN model is reliable for predicting the speed limit of cars moving on the steel girder bridge.

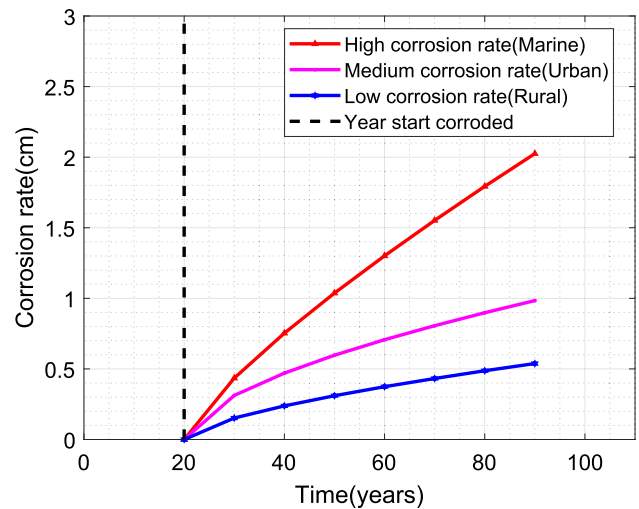


Figure 10. The corrosion rate in different environment.

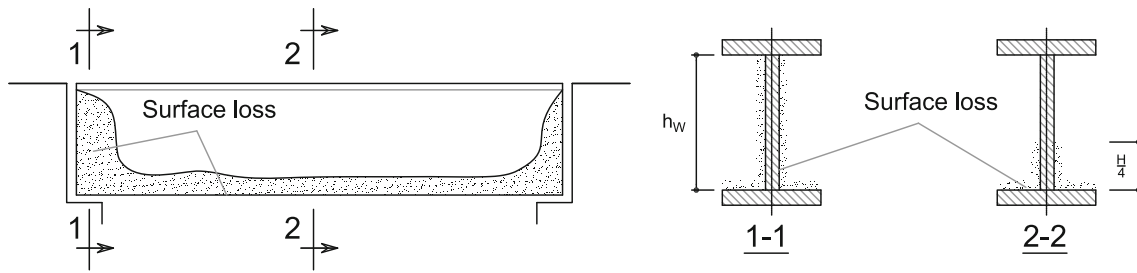
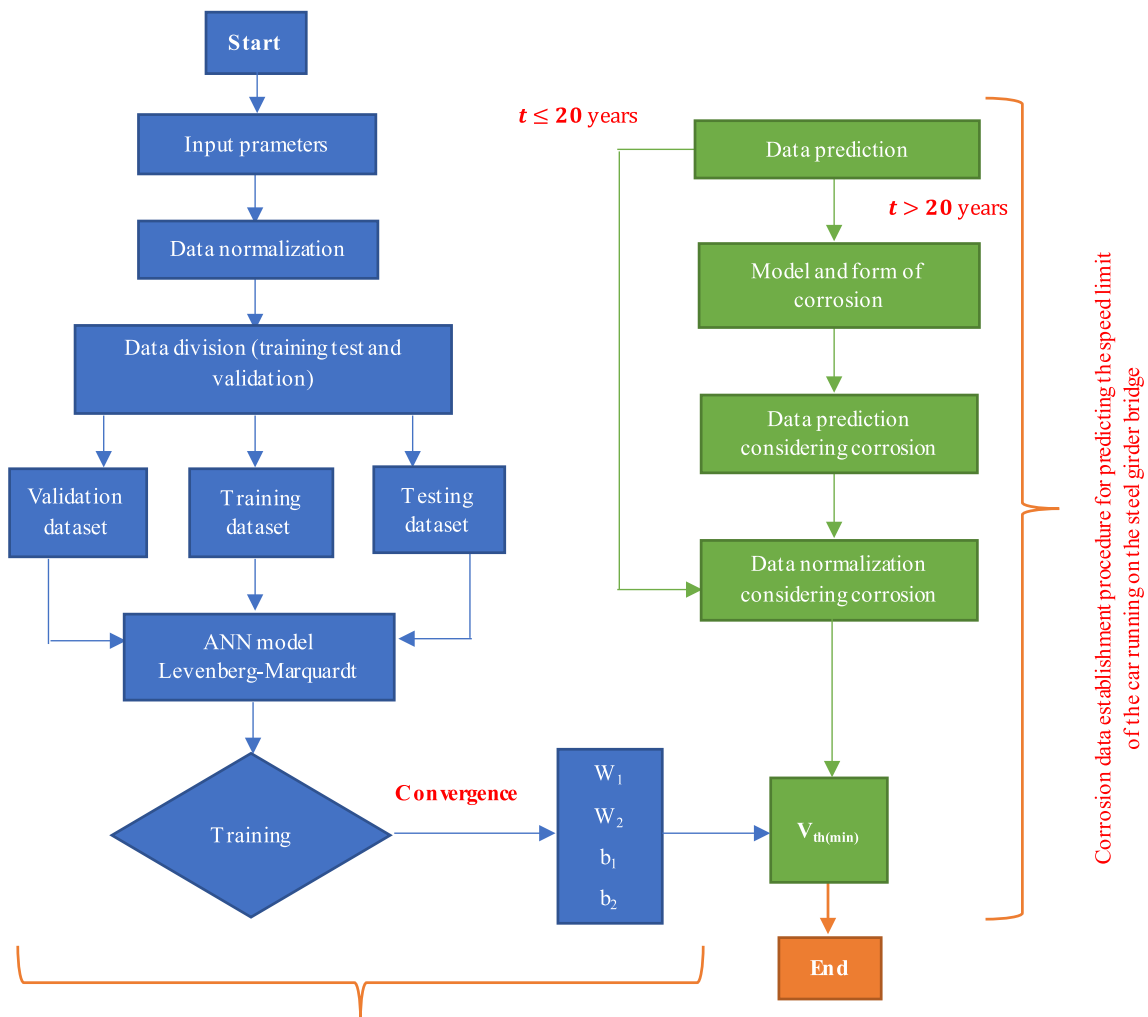


Figure 11. Corrosion form of steel girder bridges (adapted from [20]).



The implementation process of structure the ANN model for predicting the speed limit of the car running on the steel girder bridge

Figure 12. Flowchart of speed limit prediction of cars moving on the corroded steel girder bridge.

Table 4. Coefficients for Eq. (22).

i	h_i	c_{i0}	c_{i1}	c_{i2}	c_{i3}	c_{i4}	c_{i5}	c_{i6}	c_{i7}	c_{i8}	c_{i9}
0	0.3015										
1	- 1.3931	- 0.0238	0.3751	- 0.4157	1.5561	- 1.2072	- 0.6955	- 0.0704	- 0.2391	0.7842	0.0448
2	- 1.6602	- 0.0804	0.3442	0.1300	- 0.2450	0.2587	- 1.2519	0.0138	- 0.5943	1.2137	- 0.8036
3	2.0011	- 0.3371	- 0.1377	0.0110	- 0.1585	- 0.1018	- 0.3513	0.0193	1.8480	- 0.3526	0.3807
4	- 0.7266	- 0.0656	0.0628	- 0.7579	- 0.3386	0.0274	- 1.1104	- 0.3998	0.3136	- 0.0816	0.7174
5	0.0940	0.0090	- 0.7916	- 1.5721	- 0.3363	- 0.6219	- 0.7973	- 0.8906	- 0.3452	- 0.7936	- 0.2042
6	- 0.2552	- 0.0347	- 0.5393	1.1660	- 0.0222	0.0859	- 0.7037	- 0.3884	- 0.4575	0.1682	0.3502
7	- 0.3992	0.3693	0.1091	0.0015	0.1668	0.1569	0.1275	- 0.1631	- 0.3106	0.4970	- 0.5397
8	0.1210	- 0.0146	1.0016	- 0.2810	- 0.2757	0.8424	- 1.0311	- 0.6383	- 0.9408	0.0775	- 0.9622
9	- 0.8662	- 0.0222	- 0.2811	- 0.6772	0.4550	0.3323	0.2342	- 1.1052	- 1.3984	1.2266	- 1.3933
10	1.0855	- 0.1144	- 0.1745	- 0.4968	- 0.1150	0.0968	- 1.4150	- 0.5065	0.3616	- 0.1241	0.8108
11	- 1.8390	0.7831	0.1090	0.0616	0.2486	0.0362	0.5229	0.0514	- 0.3780	0.3722	- 1.6826
12	- 1.8134	- 0.0181	- 1.0853	- 0.6385	1.4064	1.2171	- 0.3039	0.0167	0.1736	0.1079	- 0.1168
13	- 1.2231	- 0.1257	- 0.2523	0.1292	0.5602	0.1014	- 0.8487	- 0.1491	- 0.6677	- 0.1366	- 1.0596
14	- 1.6357	- 0.0939	0.0663	0.0927	0.0565	- 0.1872	0.7709	0.2849	- 0.0917	- 1.4941	- 0.3859

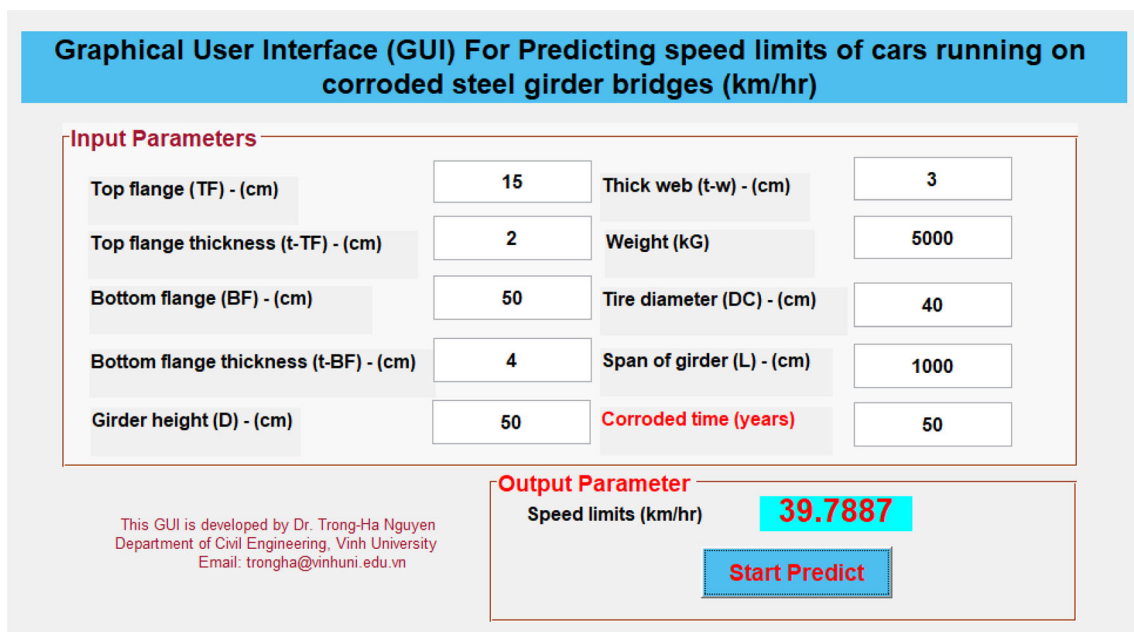


Figure 13. Graphical user interface program.

Table 5. Input parameters of the example.

TF (cm)	t-TF (cm)	BF (cm)	t-BF (cm)	D (cm)	t-w (cm)	M (kG)	DC (cm)	L (cm)
43.0	5.0	39.0	4.0	69.0	5.0	5161.0	79.0	1961.0

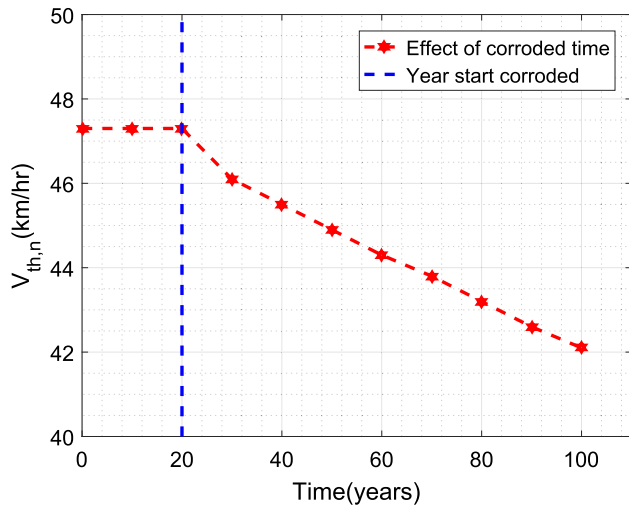


Figure 14. Time-dependent speed limit of corroded steel girder bridges.

Table 6. The databases of the input parameters.

Parameter	L	LM	M	MH	H
<i>TF</i>	15.00	28.94	42.88	56.44	70.00
<i>t-TF</i>	2.00	3.55	5.10	6.55	8.00
<i>BF</i>	15.00	27.05	39.11	57.05	75.00
<i>t-BF</i>	2.00	3.03	4.05	5.03	6.00
<i>D</i>	25.00	47.15	69.31	84.65	100.00
<i>t-W</i>	3.00	3.85	4.71	5.35	6.00
<i>M</i>	1000.00	3080.39	5160.77	6830.39	8500.00
<i>DC</i>	35.00	56.95	78.91	94.45	110.00
<i>L</i>	1000.00	1480.71	1961.41	2230.71	2500.00

Note: (L) – Low; LM – Middle low; M – Medium; MH – Middle high; H – High.

5. Speed limit prediction of cars moving on corrosive steel girder bridges

5.1 Corrosion model

Corrosion properties (e.g., section deterioration, corrosion form, and fatigue strength) are adopted from the suggestion of Nowak and Szerszen [20]. Meanwhile, the atmospheric corrosion rate of carbon steel is expressed by an exponential law suggested by Komp [1], as shown in Eq. (20).

$$R(t) = \Delta_A t^{\Delta_B} \tag{20}$$

where $R(t)$ is the mean corrosion rate (μm); t is the corrosion time (years). Δ_A and Δ_B are coefficients determined by local experimental data [1]. Three environmental conditions are considered in the model, in which marine, urban, rural areas are corresponding to the high, medium, and low corrosion rates, respectively (see table 3).

The effectiveness of protective coating is assumed until the 20th year (i.e., zero corrosion up to 20 years). The corrosion

rate curves for three environmental conditions are plotted in figure 10. The corrosion form of the steel girder bridge is adopted from the previous study [20], as shown in figure 11.

5.2 Speed limit prediction of cars moving on corroded steel girder bridges

Prediction of speed limits of cars moving on corroded steel girder bridges in this study is a combination of the corrosion rate in Eq. (20), the corrosion form shown in figure 11, and the training result of the ANN model. The flowchart of the prediction procedure is illustrated in figure 12.

Following steps are considered in predicting the speed limit of cars moving on the corroded steel girder bridge.

- *Step 1.* Determine the prediction data and corroded time.
- *Step 2.* Calculate of the area and stiffness sections loss considering corroded steel girder bridge.
- *Step 3.* Normalize the datasets.
- *Step 4.* Determine the speed limit of cars moving on the corroded steel girder bridge by combining the training results of the ANN model and the normalization data considering the corrosion.

5.3 Predictive formula for the speed limit of cars moving on the steel girder bridge

It is needed to transform the proposed ANN model to a practical formula for engineering practices. This study has proposed a formula to determine the speed limit of cars moving on a steel girder bridge based on the ANN model, expressed by.

$$V_{th(min)} = 282.68 \times \left(V_{th(min)}^N + 1 \right) + 12.10 \tag{21}$$

where the coefficients 282.68 and 12.10 are half of the maximum and minimum speed limits difference, and the minimum speed limits value of the input datasets, respectively. $V_{th(min)}^N$ is the normalized speed limits, which is determined by the following expression,

$$V_{th(min)}^N = h_0 + \sum_{i=1}^{14} h_i H_i \tag{22}$$

$$H_i = \tan h(c_{i0} + c_{i1}X_1 + c_{i2}X_2 + \dots + c_{i9}X_9)$$

where h_0, h_i and c_{i0}, \dots, c_{i9} are coefficients obtained from the ANN model and summarized in table 4.

5.4 Graphical user interface

In addition to the proposed equation, a graphical user interface programs (GUI) tool is developed based on

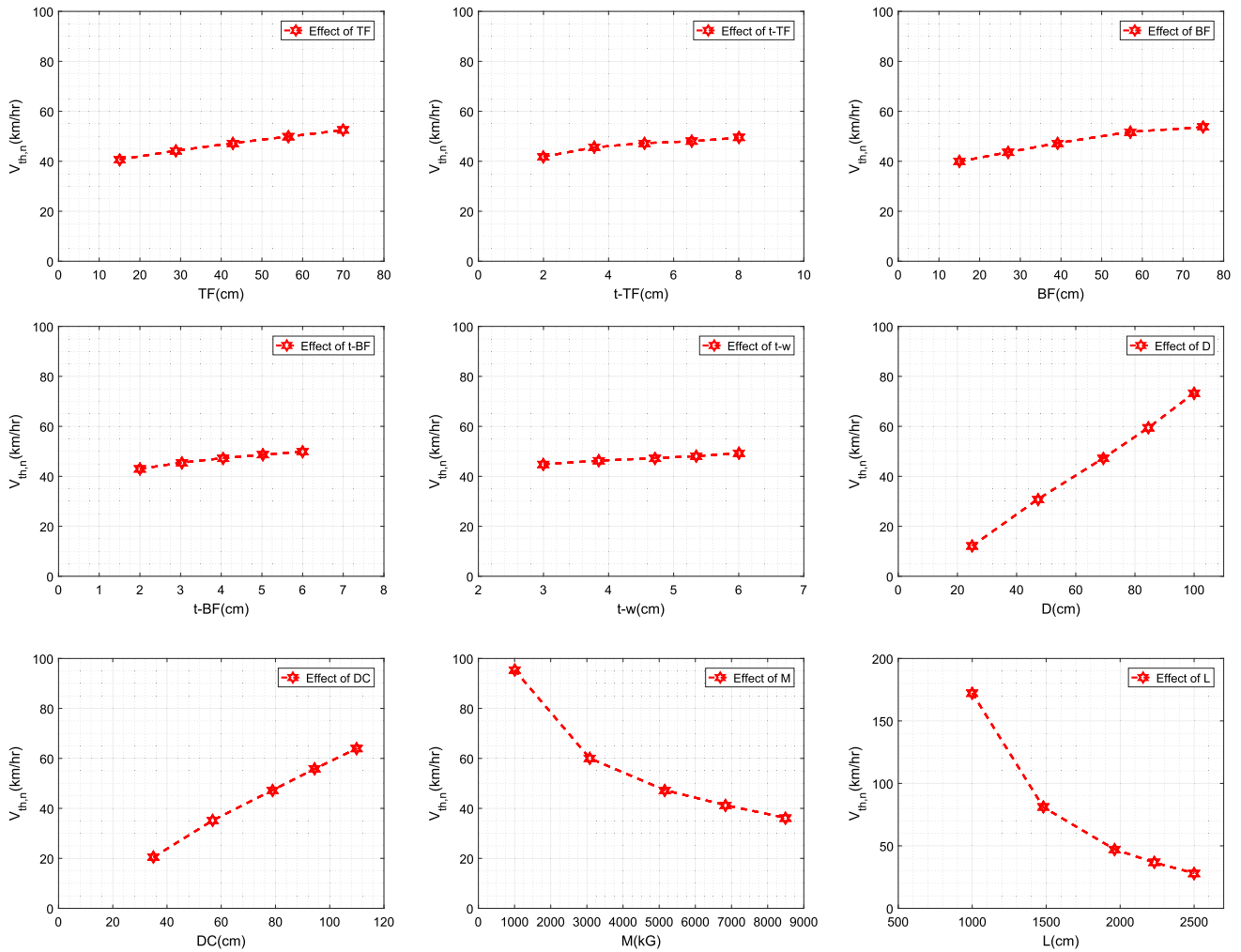


Figure 15. Effects of input parameters on the speed limits.

MATLAB [21], as shown in figure 13. It is easy to calculate the speed limits for designers and managers. Nine input variables include the car’s weight, tire diameter, and the steel girder bridge configurations, which are top flange width, top flange thickness, bottom flange width, bottom flange thickness, girder height, web thickness, the span of girder, and corrosion time. This tool is freely accessible and easy to use. The user needs to enter all the input variables and press the “Start Predict” button to be able to determine the result. This GUI tool is developed based on the proposed ANN model, therefore the accuracy of the prediction is verified and demonstrated in the previous section.

6. Number practice

Considering the single-span steel girder bridge with the load limits according to design parameters, the input parameters of the steel girder bridge are given in table 5. The service life of the steel girder bridges is considered until the 100th year, meanwhile the metal corrosion of the steel

girder starts at the 20th year. The speed limit is decreased by time, as shown in figure 14. It can be observed in figure 14 that the speed limit considering corrosion is reduced approximately 11% after 100 years, which implies a pronounced deterioration. This finding should be considered in the current design standards.

7. Effects of input parameters on the speed limits (SL)

Effects of input parameters on the speed limit of cars moving on the steel girder bridge is helpful to designers or managers in evaluating the traffic safety and traffic service life. The input parameters are changed from minimum (L) to maximum (H) bounds. At the time to assess X_i parameter, the remaining parameters are set to the medium values. All databases are shown in table 6.

Figure 15 shows the influences of the input variables on the speed limit of cars moving on the steel girder bridges. It can be seen that the $V_{th(min)}$ value tends to increase but not

much with the increment of the top flange width, top flange thickness, bottom flange width, bottom flange thickness, and web thickness. Meanwhile, the $V_{th(min)}$ value is significantly increased with the increment of the girder height and tire diameter. By contrast, the speed limit $V_{th(min)}$ is reduced as the car's weight and girder span increased.

8. Conclusions

This study develops an ANN model to predict the speed limit of cars moving on the steel girder bridges considering metal corrosion based on 311 datasets. A procedure to determine the speed limit considering metal corrosion is proposed based on the training results of the ANN model combined with the corrosion form. The following conclusions are obtained.

- The proposed ANN model based on 311 datasets predict the speed limit of cars moving on the corroded steel girder bridges accurately with R^2 larger than 0.97 and $a20$ -index larger than 0.85.
- A practical equation for predicting the speed limit of cars moving on the corroded steel girder bridge is proposed.
- The graphical user interface program is also developed based on MATLAB, which has been freely available for designers and practitioners.
- The effects of input parameters on the speed limits of cars moving on the corrosive steel girder bridges are evaluated. The girder height and tire diameter are influential parameters, meanwhile, the car's weight and girder span have negative effects on the speed limit.

Declaration

Conflict of interest The authors declare that they have no conflicts of interest.

References

- [1] Komp M 1987 Atmospheric corrosion ratings of weathering steels-calculation and significance. *Mater. Perform.* 26: 42–44
- [2] Landolfo R, Cascini L and Portioli F 2010 Modeling of metal structure corrosion damage: A state of the art report. *Sustainability* 2: 2163–2175
- [3] Secer M and Uzun E T 2017 Corrosion damage analysis of steel frames considering lateral torsional buckling. *Procedia Eng.* 171: 1234–1241
- [4] Nguyen T H, Nguyen D D 2020 Reliability Assessment of Steel-Concrete Composite Beams considering Metal Corrosion Effects. *Adv. Civ. Eng.* 2020
- [5] Tran N L, Nguyen T H 2021 Effect of Metal Corrosion on the Structural Reliability of the 3D Steel Frames. In: *Proceedings of the 3rd International Conference on Sustainability in Civil Engineering*, 39–44 Springer
- [6] Ngoc-Long T and Ha T 2020 The effect of metal corrosion on the structural reliability of the Pre-Engineered steel frame. *J. Mater. Eng. Struct.* 7: 155–165
- [7] Ha N T 2019 Reliability assessment of frame steel considering semi-rigid connections. *J. Mater. Eng. Struct.* 6: 119–126
- [8] Tran V L, Thai D K and Nguyen D D 2020 Practical artificial neural network tool for predicting the axial compression capacity of circular concrete-filled steel tube columns with ultra-high-strength concrete. *Thin-Walled Struct.* 151: 106720
- [9] Lim S and Chi S 2021 Damage Prediction on Bridge Decks considering Environmental Effects with the Application of Deep Neural Networks. *KSCE J. Civ. Eng.* 25: 371–385
- [10] Tran V L and Kim S E 2021 A practical ANN model for predicting the PSS of two-way reinforced concrete slabs. *Eng. Comput.* 37: 2303–2327
- [11] Khajehei H, Ahmadi A, Soleimanmeigouni I, Haddadzade M, Nissen A and Latifi Jebelli M J 2022 Prediction of track geometry degradation using artificial neural network: A case study. *Int. J. Rail Transp.* 10: 24–43
- [12] Zou Q, Jiang H, Dai Q, Yue Y, Chen L and Wang Q 2019 Robust lane detection from continuous driving scenes using deep neural networks. *IEEE Trans. Veh. Technol.* 69: 41–54
- [13] Tran-Ngoc H, Khatir S, De Roeck G, Bui-Tien T and Wahab M A 2019 An efficient artificial neural network for damage detection in bridges and beam-like structures by improving training parameters using cuckoo search algorithm. *Eng. Struct.* 199: 109637
- [14] Dougherty M 1995 A review of neural networks applied to transport. *Transp. Res. Part C: Emerging Technol.* 3: 247–260
- [15] Kikuchi S, Nanda R and Perincherry V 1993 A method to estimate trip O-D patterns using a neural network approach. *Transp. Plann. Technol.* 17: 51–65
- [16] Yang H, Akiyama T, Sasaki T 1992 A neural network approach to the identification of real time origin-destination flows from traffic counts. In: *International Conference on Artificial Intelligence Applications in Transportation Engineering*, San Buenaventura, California, USA
- [17] Kaseko M S and Ritchie S G 1993 A neural network-based methodology for pavement crack detection and classification. *Transp. Res. Part C: Emerging Technol.* 1: 275–291
- [18] Mead W C, Fisher H N, Jones R D, Bisset K R, Lee L A 1993 *Application of adaptive and neural network computational techniques to traffic volume and classification monitoring*. Los Alamos National Lab., NM (United States)
- [19] Nakatsuji T and Kaku T 1991 Development of a self-organizing traffic control system using neural network models. *Transp. Res. Rec.* 1324: 137–145
- [20] Nowak A S and Szerszen M M 2001 Reliability profiles for steel girder bridges with regard to corrosion and fatigue. *J. Theor. Appl. Mech.* 39: 339–352
- [21] Mathworks 2018 MATLAB and statistics toolbox release 2018b. Natick, Massachusetts, United States
- [22] Nguyen T H, Tran N L and Nguyen D D 2022 Prediction of Axial Compression Capacity of Cold-Formed Steel Oval Hollow Section Columns Using ANN and ANFIS Models. *Int. J. Steel Struct.* 22(1): 1–26
- [23] Nguyen T H, Tran N L and Nguyen D D 2021 Prediction of Critical Buckling Load of Web Tapered I-Section Steel

- Columns Using Artificial Neural Networks. *Int. J. Steel Struct.* 21(4): 1159–1181
- [24] Zorlu K, Gokceoglu C, Ocakoglu F, Nefeslioglu H and Acikalin S 2008 Prediction of uniaxial compressive strength of sandstones using petrography-based models. *Eng. Geol.* 96: 141–158
- [25] Nguyen D D, Tran V L, Ha D H, Nguyen V Q and Lee T H 2021 A machine learning-based formulation for predicting shear capacity of squat flanged RC walls. *Structures* 29: 1734–1747
- [26] Patel V M and Mehta H B 2018 Thermal performance prediction models for a pulsating heat pipe using Artificial Neural Network (ANN) and Regression/Correlation Analysis (RCA). *Sādhanā* 43: 1–16
- [27] Patil S B and Subbareddy N 2002 Neural network based system for script identification in Indian documents. *Sadhana* 27: 83–97
- [28] Nikbin I M, Rahimi S and Allahyari H 2017 A new empirical formula for prediction of fracture energy of concrete based on the artificial neural network. *Eng. Fract. Mech.* 186: 466–482
- [29] Golafshani E M and Ashour A 2016 A feasibility study of BBP for predicting shear capacity of FRP reinforced concrete beams without stirrups. *Adv. Eng. Software* 97: 29–39